Received 29 April 2005
Revised 24 November 2005
Accepted 5 December 2005

Modelling ice melting processes: numerical and experimental validation

Marcela Cruchaga and Diego Celentano
Departamento de Ingeniería Mecánica, Universidad de Santiago de Chile, Santiago, Chile

Abstract

Purpose – This work is devoted to the experimental analysis, numerical modelling and validation of ice melting processes.

Design/methodology/approach – The thermally coupled incompressible Navier-Stokes equations including water density inversion and isothermal phase-change phenomena are assumed as the governing equations of the problem. A fixed-mesh finite element formulation is proposed for the numerical solution of such model. In particular, this formulation is applied to the analysis of two different transient problems.

Findings – The numerical results computed with the finite element formulation have been found to be very similar to the corresponding predictions, also obtained in this study, provided by a finite volume enthalpy-based technique. Both numerical results, in turn, satisfactorily approached the available experimental measurements expressly conducted in the context of this work for validation purposes.

Research limitations/implications – They are mainly due to some model simplifications (e.g. no volume changes are considered during the solid-liquid transformation) and to the inherent difficulties associated with the experimental measurements.

Practical implications – This study may be relevant for a better understanding of the phenomena occurring in different engineering applications involving phase-change in water: food freezing, ice formation in pipes, freezing/melting processes in soils, ice growth in plane wings, etc.

Originality/value – The study is mainly focused on the validation of the numerical predictions obtained with the finite element formulation mentioned above with other results provided by a well-known finite volume technique and, in addition, with available laboratory measurements carried out in the context of this work.

Keywords Modelling, Numerical analysis, Water, Freezing, Melting

Paper type Technical paper

Nomenclature

Ω = arbitrary open bounded domain ($\Omega = \Omega_l \cup \Omega_s$)
Γ = smooth external boundary of Ω
Ω_l = time-varying liquid (water) domain
Ω_s = time-varying solid (ice) domain
Y = time interval of interest ($t \in Y$)
ρ = density
μ = dynamic viscosity
$\mathbf{v}$ = velocity vector
p = pressure

International Journal of Numerical Methods for Heat & Fluid Flow
Vol. 17 No. 5, 2007
pp. 548-564

0961-5539
DOI 10.1108/09615530710753008

The supports provided by the Chilean Council for Research and Technology CONICYT (FONDECYT Projects No. 1020029 and No. 1030209) and the Department of Technological and Scientific Research at the Universidad de Santiago de Chile are gratefully acknowledged.

$\mathbf{b}$ = specific body force vector
$\boldsymbol{\varepsilon}$ = rate of deformation tensor
T = temperature
C = specific heat capacity
L = specific latent heat
K = isotropic thermal conductivity
f_{pc} = phase-change function
∇ = spatial gradient operator
$\dot{(\,)}$ = time derivative of ()

1. Introduction

The proper description of many industrial applications like refinement of metals, casting or freezing procedures requires the analysis of phase-change phenomena involving convective effects. The analysis of such complex problems can be performed through physical scaled models aimed at providing valuable experimental data that allow, in turn, to achieve a better understanding of the process and, eventually, to evaluate particular engineering requirements. Usually, this information is more easily obtained in such a form than from the real situation. On the other hand, the numerical modelling is an alternative option to analyse several processes involving thermally coupled flows with phase-change since computational simulations are now-a-days recognised as powerful tools that may help to predict physical behaviours and to identify mechanisms that appear in the different applications. Nevertheless, these numerical analyses present difficulties related to mathematical and computational aspects that have led, during the last years, to the development of robust formulations with the corresponding numerical assessment and experimental validation of their predictions (Brent *et al.*, 1988; Cruchaga and Celentano, 2001; Dantzig, 1989; Khodadadi and Zhang, 2001; Lacroix and Voller, 1990; Lewis and Ravindran, 2000; McDaniel and Zabaras, 1994; Swaminathan and Voller, 1993; Webb and Viskanta, 1986 and references therein).

In particular, the study of phase-change in water is relevant in different engineering applications: food freezing, ice formation in pipes, freezing/melting processes in soils, ice growth in plane wings, etc. Therefore, many authors have been devoted their efforts to specifically analyse the natural convection in water evaluating the effect of density inversion as well as its interaction with the ice melting process (Ishikawa *et al.*, 2000; Rieger and Beer, 1986; Tsai *et al.*, 1998; Yamada *et al.*, 1997).

In this work we present a thermally coupled flow modelling of ice melting processes. The aim of this study is the assessment of the performance of the fixed-mesh finite element temperature-based (FE-TB) formulation proposed by Cruchaga and Celentano (2001) when density inversion and isothermal phase-change phenomena are considered. To this end, the corresponding numerical predictions are compared with other results also computed in this work using a well-known finite volume enthalpy-based technique and, in addition, with available laboratory measurements carried out in the context of the present research. The governing differential equations (linear momentum, continuity and energy) are presented in Section 2 together with a brief description of the two referred fixed-grid techniques, respectively, developed in the contexts of the finite element and finite volume methods. These methodologies are applied in the analysis of two ice melting problems described in Section 3. Special attention is given to the numerical assessment and experimental validation of the computed results. Finally, the effects of natural convection and heat transfer conditions on the flow response are also discussed.

2. Governing equations and discrete models

In the present analysis, the description of ice melting process in water is assumed to be given by the incompressible Newtonian laminar flow equations in addition to the heat transfer balance as:

- equation of motion:

$$\rho\dot{v} + \rho(v\cdot\nabla)v + \nabla p - \nabla(2\mu\varepsilon) = \rho b \quad \text{in } \Omega_l \times \Upsilon \tag{1}$$

- continuity equation:

$$\nabla\cdot v = 0 \quad \text{in } \Omega_l \times \Upsilon \tag{2}$$

- energy equation:

$$\rho\left(c + L\frac{\partial f_{pc}}{\partial T}\right)\left(\dot{T} + v\cdot\nabla T\right) = \nabla(k\nabla T) \quad \text{in } \Omega \times \Upsilon \tag{3}$$

together with adequate (standard) boundary and initial conditions and an appropriate constitutive relationship for the phase-change function f_{pc} (Cruchaga and Celentano, 2001). The constitutive model for the isothermal phase-change function considered in this work to represent the phase-change behaviour of water is chosen as the temperature-dependent Heaviside function written in terms of the melting temperature T_m as $f_{pc} = H(T - T_m)$. This definition leads to $f_{pc} = 0$ and $f_{pc} = 1$ in the solid and liquid phases, respectively, (i.e. $f_{pc} = 0$ in Ω_s and $f_{pc} = 1$ in Ω_l).

The water density inversion phenomenon is taken into account in the specific body force vector expression $\mathbf{b} = \mathbf{g}f_\alpha$, where $\mathbf{g}$ is the gravity acceleration vector and $f_\alpha(T)$ is the buoyancy factor. Additionally, temperature-dependent dynamic viscosity, specific heat capacity and thermal conductivity are considered in the present model.

It should be noted that equations (1) and (2) are, in fact, only solved in the liquid domain since the solid region is assumed to be fixed (i.e. a zero velocity field is adopted for this phase). In contrast, the energy equation (3) is computed in the whole domain Ω considering a continuous temperature field. Therefore, this model describes a purely thermal conductive behaviour for the solid phase. Moreover, the effect of the latent heat release occurring at the phase-change (ice-water) interface is, as reported in Cruchaga and Celentano (2001), implicitly incorporated in the function f_{pc}, i.e. the classical Stefan phase-change boundary condition is embedded in the thermal balance given by equation (3). This interface is considered as an internal boundary where the fluid velocity is prescribed to zero.

2.1 Finite element temperature-based model (FE-TB)

The non-isothermal incompressible Navier-Stokes set of equations (1)-(3) is discretized within the context of the finite element method by using a generalized streamline operator technique. This fixed-mesh finite element thermally coupled flow formulation including phase-change effects has been previously presented in Cruchaga and Celentano (2001). The related variational formulation, which enables the use of equal order interpolation functions for the nodal unknowns, intrinsically provides some stabilization terms aimed at improving the numerical response for dominant

convection problems and, additionally, it does not need tuning parameters chosen outside the model in the definition of the upwinding coefficients. On the other hand, the latent heat effects are taken into account through a temperature-based model able to deal with either isothermal or non-isothermal phase-changes. For the isothermal phase-change problem particularly studied in this work, the discontinuity of f_{pc} existing at the liquid-solid interface is circumvented in the corresponding weak form by using a boundary integral over such front that properly captures the latent heat release (further details can be found in Celentano, 1998). Moreover, the temporal discretization of the unknowns is performed using an Euler backward scheme. This methodology is not restricted to structured meshes and can directly be applied to 3D problems.

The resulting strongly coupled system of discretized equations is solved via a staggered scheme that preserves the coupling degree given by the energy transport terms and the temperature-dependent flow properties. In this framework, due to the high nonlinearity present in this formulation, the computational solution of the fluid dynamics and heat transfer problems is carried out using a Newton-Raphson type algorithm.

2.2 Finite volume enthalpy-based model (FV-HB)

In this case, the set of equations (1)-(3) is discretized using a staggered grid in which the pressure and temperature are computed at the center node of the cell whereas the velocity and heat flux are evaluated at the cell's faces. Linear interpolation functions are used for these variables in the calculation of viscous forces and conduction heat fluxes. Moreover, the power law differencing scheme is considered to calculate the convective terms (FLUENT, 1999).

In this context, the energy equation (3) is written in terms of the enthalpy where the phase-change is assumed to occur in a small temperature range $[T_{\mathrm{m}} - T_{\mathrm{m}}/2;\ T_{\mathrm{m}} + T_m/2]$ (ΔT_m is chosen as 0.2°C in the problems of Section 3). Details about the procedure to handle the inherent nonlinearity of the phase-change energy term can be found in Brent *et al.* (1988), Lacroix and Voller (1990) and Swaminathan and Voller (1993).

The resulting algorithm solves in a sequential way the linear momentum, continuity and energy discretized equations. Moreover, under-relaxation is applied during the iterative procedure (FLUENT, 1999). In the simulations carried out in this work, the under-relaxation factor for the velocity components and pressure is around 0.1 while that for the temperature ranges between 0.6 and 0.8.

The performance of both models (referred as FE-TB and FV-HB from here onwards) is assessed in the analysis of the problems presented in Section 3.

3. Numerical and experimental validation: results and discussion

Two different melting processes of ice are presented in this section. The aims of the present analyses are: to describe the influence of both buoyancy effects and different heat transfer boundary conditions on the numerical responses predicted by the FE-TB model, to assess these results with those obtained with the FV-HB method and, finally, to compare both simulations with some available experimental measurements.

As already mentioned, the buoyancy effects developed under the gravity action ($g = 9.8\,\mathrm{m/s^2}$) are described in the simulations by using a temperature-dependent

factor $f_\alpha(T)$ able to deal with the water inversion effect ($1/f_\alpha = 1.0 + A_1 T + A_2 T^2 + A_3 T^3 + A_4 T^4$ with $A_1 = -0.6789 \times 10^{-4}, A_2 = 0.9073 \times 10^{-5}, A_3 = -0.9646 \times 10^{-7}$, $A_4 = 0.8737 \times 10^{-9}$ where T is expressed in °C). The temperature relationships for different properties in the liquid phase (buoyancy factor, dynamic viscosity, specific heat capacity and thermal conductivity) are shown in Figure 1 (Ishikawa *et al.*, 2000). The specific heat capacity and thermal conductivity in the solid phase are taken as constants with values corresponding to those at 0°C of the $c - T$ and $k - T$ curves, respectively. The latent heat considered in the study is $L = 335{,}000$ J/kg with a melting temperature $T_m = 0$°C. The density is assumed constant and equal in both phases with the value $\rho = 999.8395\,\text{kg/m}^3$ (i.e. for simplicity, the effect of density change between ice and water is not included in the analysis).

3.1 Melting of ice inside a horizontal cylinder

This problem, exhaustively analysed in Rieger and Beer (1986), is presented here to assess the performance of the FE-TB formulation by illustrating the effect of density inversion on the response of the system. Moreover, these results are compared with those also computed in the context of the present work using the FV-HB technique. The problem is schematically shown in Figure 2. The ice is initially at rest and occupies the whole domain. In the computations, the ice (solid material) is fixed at the center of the cylinder. The initial temperature of the rod is -0.01°C, the cylinder has a radius $R_0 = 0.03$ m and the prescribed temperature at the wall is assumed constant as $T_w = 6$°C. In this configuration, the rod of ice is expected to reduce its diameter ($2R_0$) as it melts. Nevertheless, as observed in the experiments reported in Rieger and Beer (1986), such reduction was found not to be the same along different radial lines due

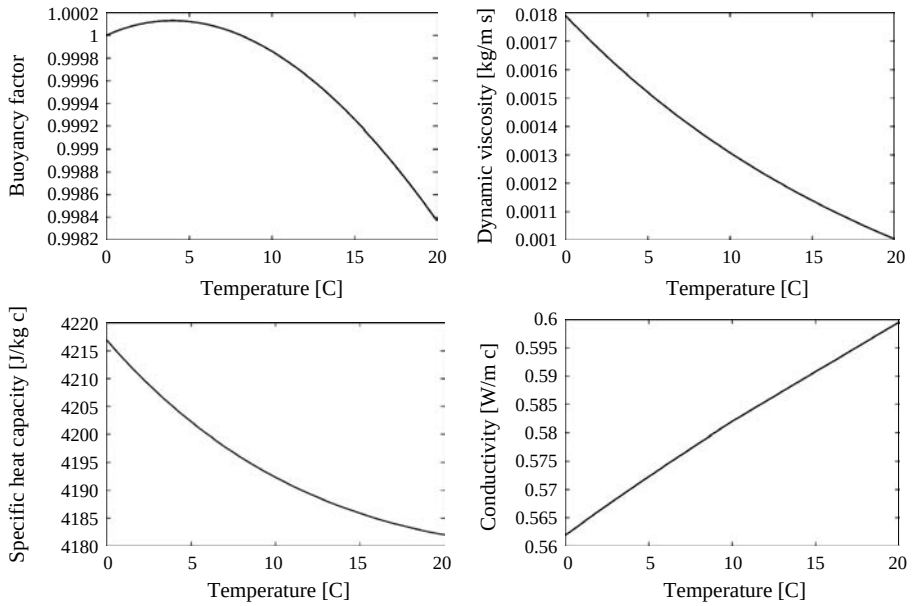

Figure 1.
Temperature-dependent properties of water

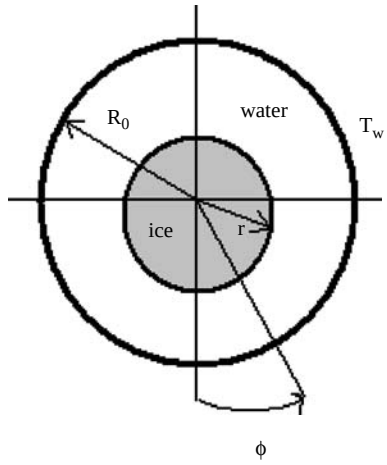

Figure 2.
Melting of ice inside a horizontal cylinder: problem description

to the presence of natural convection with density inversion that develops during the process.

The same spatial and time discretizations were used for the FE and FV computations. Owing to symmetry, half of the domain has been considered and meshed with approximately 5,000 four-noded isoparametric elements (using 90 elements in the radial direction with a non-uniform distribution to properly describe the strong velocity and temperature gradients expected near the wall: 15 elements for the radius interval [0.0;0.015 m] and 75 elements for [0.015;0.030 m]). The adopted time step was 20 s.

In order to evaluate the effect of density inversion on the melting evolution, a preliminary simulation is performed considering the classical Boussinesq approach given by a linear approximation of the buoyancy factor $f_\alpha = 1 - \alpha T$, with $\alpha = 1.1 \times 10^{-4}$°C^{-1} being the secant (between 4 and 20°C) volumetric expansion coefficient. In this case, the Stefan ($Ste = c(T_w - T_m)/L$), Rayleigh ($Ra = g\alpha(T_w - T_m)R_0^3\rho^2 c/(\mu k)$) and Prandtl ($\Pr = \mu c/k$) numbers are 0.075, 8.7×10^5 and 10.8, respectively, (μ, c and k evaluated at 6°C). The isotherms and streamlines computed with the FE-TB model are shown in Figure 3. The strong thermally induced flow motion is apparent. This fact is also reflected in the ice radius reduction (r/R_0, r being the instantaneous radius) history curve shown in Figure 4. It is seen that the greater reductions occur at the upper face of the ice. Moreover, a pure conduction heat transfer analysis has also been performed for comparison purposes (note that in this last case the radius reduction evolution is independent of the angle ϕ). Clearly, the natural convection promotes higher cooling rates that can be appreciated in the more advanced positions of the corresponding phase-change front with respect to those computed using the pure heat conduction model.

Figure 5 shows the isotherms and streamlines obtained with the FE-TB model considering density inversion. This effect provides smoother results than those of Figure 3 owing to the smaller characteristic lengths (along the radial direction in this case) of the regions in which the several vortexes develop. The radius reduction histories of the interface position plotted in Figure 6 exhibit similar responses for the different orientations. A slower phase-change interface evolution is observed in comparison with that of Figure 4. Moreover, unlike the results obtained with the

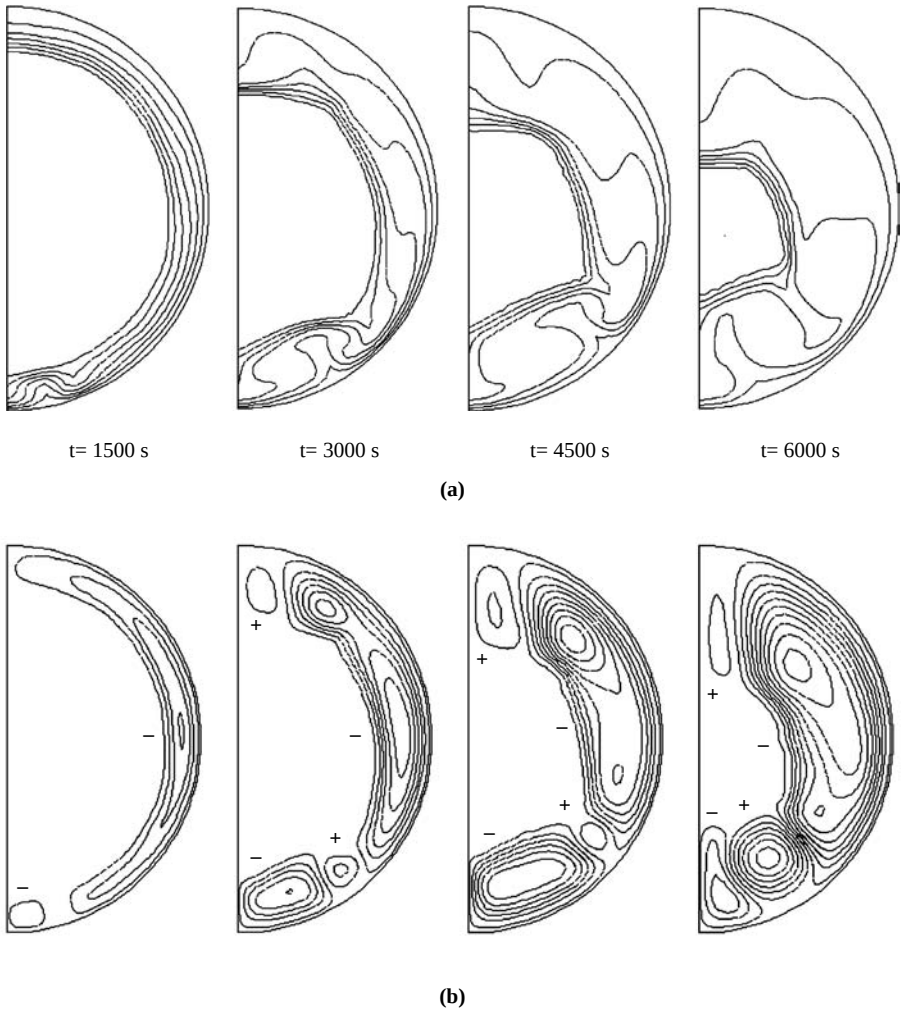

Figure 3.
Melting of ice inside a horizontal cylinder

Notes: FE-TB results obtained with a linear (Boussinesq type) buoyancy factor. (a) Isotherms (plotted 1ºC apart from T_w = 6ºC) and (b) streamlines (plotted $5x10^{-7}$ m^2/s apart; clockwise + and anti-clockwise –) at different times of the analysis

Boussinesq approximation, the density inversion causes the occurrence of greater reductions at the lower face of the ice.

Figure 7 shows the FE-TB and FV-HB solutions for the ice radius evolution together with the corresponding experimental measurements reported by Rieger and Beer (1986). A very good agreement between both formulations can be observed (although not shown, satisfactory fittings were also obtained for the results corresponding to the pure conduction model and the Boussinesq simulation). In addition, it is seen that the numerical solutions approximately adjust the measurements. Finally, it is

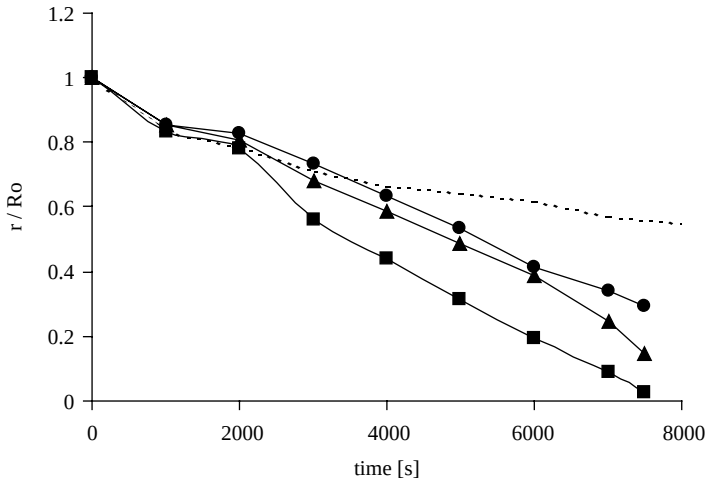

Notes: FE-TB results obtained with a linear (Boussinesq type) buoyancy factor for the radius evolution at 0º (●), 90º (▲) and 180º (■). The results computed with a pure heat conduction model are plotted in dashed lines

Figure 4.
Melting of ice inside a horizontal cylinder

important to remark that all the trends appreciated in Figures 5-7 are in good comparison with the numerical results presented by Rieger and Beer (1986).

3.2 Melting of a square rod of ice immersed in water

An experimental and numerical study of an ice melting process developed in a water environment is presented. A rod of ice ten times longer than the horizontal side of its transversal square section was submerged in a box of glass filled with water in order to reproduce conditions closer to a two dimensional situation at the middle transversal section. The dimensions of the rod and box are shown in Figure 8(a). The thermocouples (type T, copper-constantan with diameter 0.0015 m) were positioned in the middle-transversal plane as shown in Figure 8(b). Thermocouple 11 served as environmental temperature controller. The measurements taken from thermocouples 1, 8, 10, 14 and 15 contributed to evaluate the effect of the heat transfer along the water interface and the glass walls. All the thermocouples were calibrated with a digital thermometer where the average error in the measurements was estimated as ± 0.5°C. The ice rod was frozen during almost 5 h at a temperature low enough to produce a uniform and complete solidification and, additionally, to avoid a crack due to a thermal shock when the rod was immersed in the water. A set of nearly 20 experiments were carried out but only eight were accepted considering a reasonable recurrence in the following aspects: initial air and water temperatures, a nearly square initial rod section with a maximum admissible error of ± 0.002 m in its height (this error corresponds to 7 per cent of the initial section) and the permanence of the rod in the correct position during the test (evaluated through a visual observation confirmed by similar temperature evolutions registered by the thermocouples symmetrically located). According to that, only the measurements taken during the first 4 min were considered. One of the experiences that satisfied all the mentioned conditions is reported in the present work. The initial section of the rod was 0.03 m wide and 0.028 m

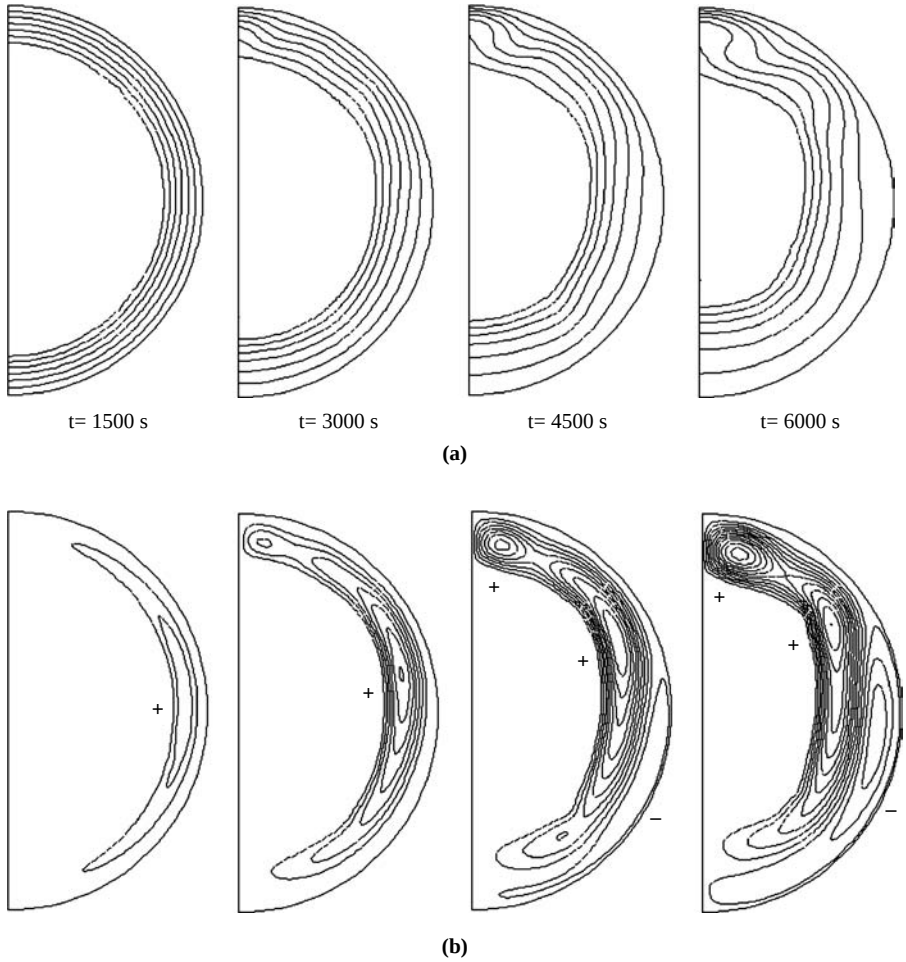

Figure 5.
Melting of ice inside a horizontal cylinder

Notes: FE-TB results obtained with a fourth order buoyancy factor (accounting for density inversion). (a) Isotherms (plotted 1ºC apart from T_w = 6ºC) and (b) streamlines (plotted $1x10^{-7}$ m^2/s apart; clockwise + and anti-clockwise –) at different times of the analysis

height with a temperature of − 4.3°C, the environmental temperature was 25.9°C and the initial water temperature was 14.7°C. The final transversal section of the rod experienced a reduction of approximately 30 per cent. The temperature measurements are shown in Figure 9. Similar evolutions in points symmetrically located have been observed (not shown). Moreover, the greater temperature variations occur in those regions close to the ice in the bottom of the cavity. The temperature evolutions corresponding to thermocouples 9, 12 and 13 are not shown since they did not exhibit significant variations during the analysis like the responses found for points 1, 2, 7 and 8. The unexpected temperature behaviour registered by thermocouple 16 situated in the center of the ice rod denotes a localised early melting process in the vicinity of the

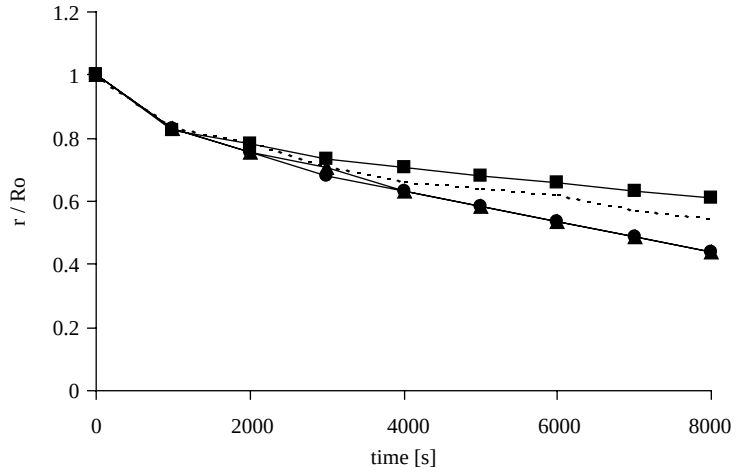

Notes: FE-TB results obtained with a fourth order buoyancy factor (accounting for density inversion). Radius evolution at 0º (●), 90º (▲) and 180º (■). The results computed with a pure heat conduction model are plotted in dashed lines

Figure 6.
Melting of ice inside a horizontal cylinder

thermocouple tip due to metal-ice contact effects. This undesirable response could have been minimise by using thinner wires. Further details of the experimental procedure can be found in Cruchaga and Celentano (2005).

This problem was simulated with the same ice and water material properties used in the former problem. The initial water and environmental temperatures considered in the computations were 15 and 26°C, respectively. Non-slip conditions on both the glass walls and the ice-water interface were considered. Owing to symmetry, only a half of the domain shown in Figure 8(b) was analysed. The finite element mesh was composed of 80 × 80 uniformly distributed standard four-noded elements. The time step size used was 0.5 s.

Three different cases were studied: a purely conductive model (case A) and a natural convection analysis (case B) both with adiabatic boundaries and, in addition, a natural convection system considering heat transfer effects in the cavity walls (case C). For case C, a heat transfer coefficient of 250 $W/m^{2o}C$ has been chosen as a boundary condition representing the glass walls conduction with a thickness of 0.004 m. For simplicity, this case has been studied adopting the same heat transfer conditions for the top boundary (free surface of water). Although the models behind the first two cases (A and B) involve simplified physical mechanisms and, therefore, no realistic predictions can be a priori expected from them, their computations are useful to quantitatively assess the influence of two particular aspects which are difficult to estimate from the experiments: fluid convection and heat flux across the external boundaries.

Experimental and FE-TB results for the temperature evolutions at different points are shown in Figure 9. The decreasing experimental evolutions registered by thermocouples 6 and 18 together with the nearly constant temperature histories at thermocouples 5 and 7 denote the presence of other heat transfer mechanisms than purely thermal conduction. The similar variations observed in thermocouples 6 and 18 make evident the development of natural convection in the bottom of the cavity.

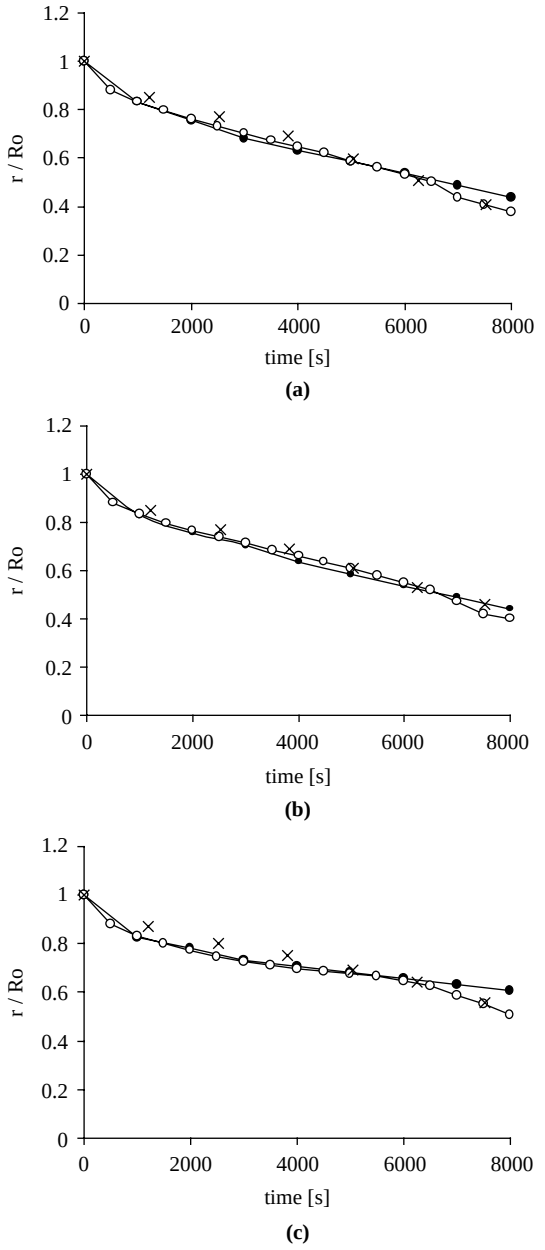

Notes: Radius evolution (including density inversion) at (a) 0º, (b) 90º and (c) 180º obtained with FE-TB (●) and FV-HB (○) models together with the experimental measurements (×) reported by Rieger and Beer (1986)

Figure 7.
Melting of ice inside a horizontal cylinder

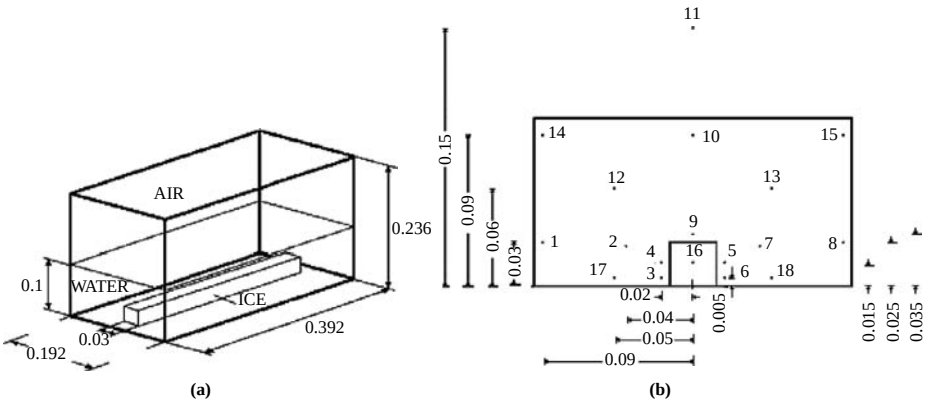

Note: dimensions in m

Figure 8.
Melting of a square rod of ice immersed in water: experimental set-up. (a) Geometry and (b) thermocouple layout

The heat flux through the boundary may be, as a preliminary approach, considered negligible based on the steady temperature recorded by thermocouple 8. Therefore, the natural convection effects are firstly evaluated by comparing the numerical responses corresponding to cases A and B.

The numerical results for the purely conductive model with adiabatic walls (case A) exhibit practically the same temperature evolutions for points 5 and 6 with large reductions of their values with respect to the initial ones. A constant temperature history is obtained for points 7, 8 and 18 showing that the heat flux does not reach their positions during the analysis. Moreover, the temperature evolutions predicted for this case present a significant discrepancy with the measurements (see, e.g. points 5, 6 and 18). On the other hand, the analysis including natural convection with adiabatic walls (case B) shows that the fluid motion induced by buoyancy effects mainly affects the temperature evolutions at points 5 and 18. At point 5, which shows temperatures greater than those predicted in case A, the hot fluxes promoted by convection partially compensate the cooling effect caused by the ice melting. Nevertheless, the temperature discrepancy between the numerical and experimental results is not diminished by this mechanism. The temperature reduction experienced by point 18 reflects a dominant convective response in this region in sharp contrast to the constant value found for case A. Although the numerical trend agrees with the measurements at this point, the temperature predictions decrease more drastically than the experimental values. Furthermore, note that the temperature evolution of point 6 qualitatively adjusts the results of case A but with lower values for advanced times of the analysis.

Owing to the numerical-experimental discrepancy observed in the previous cases, the effects of the heat transfer along the glass walls are additionally taken into account in the simulation (case C). The corresponding results, also shown in Figure 9, satisfactorily agree with the experimental measurements, in particular at thermocouples 5, 7 and 8. The temperature evolution predicted at thermocouple 6 shows a good description of the physical trend while the numerical results for thermocouple 18 reasonably represent the experimental data, mainly at the end of the analysis. The influence of the inward heat flux along the external boundaries is apparent on the temperature histories at points 5, 6 and 18. In addition, as commented

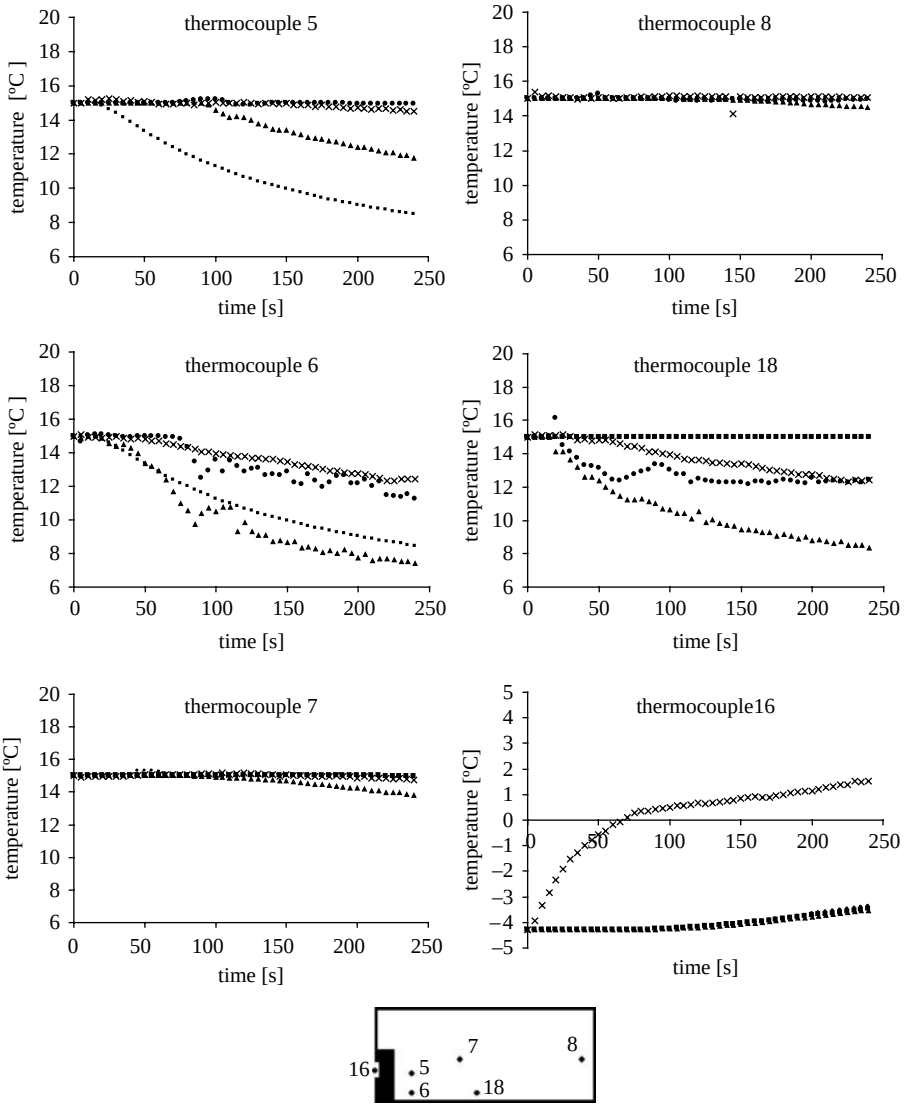

Figure 9.
Melting of a square rod of ice immersed in water

Notes: experimental (×) and FE-TB results for the temperature evolutions for cases A (■), B (▲) and C (●)

above, it is seen that the simulation does not capture the local melting produced in the vicinity of the thermocouple 16.

Although the results computed for case C are close to the experimental data, numerical oscillations remain in the predictions. This fact is directly attributable to the high level of fluid convection present in this simulation. The temperature evolution at

points situated near the ice and the bottom of the cavity denotes a slightly oscillatory behaviour that reflects the development of an incipient transitional flow regime during the melting process. It should be also noted that the heat flux discontinuity existing at the liquid-solid interface, which corresponds to the isothermal phase-change considered in the analysis, introduces instabilities in the numerical solution. One possible option to avoid this problem would consist in the dynamic enhancement of the interpolation of the variables (velocity, pressure and temperature) in regions close to such moving interface. It should be mentioned that simple mesh and time step refinements could not overcome this drawback since similar results to those computed for case C have been obtained with a numerical analysis using a non-uniform mesh of 100×160 elements (refined near the bottom of the cavity) and a smaller time step of 0.1 s (results not shown).

FE-TB results for the phase-change front position, isotherms and streamlines computed for case C are shown in Figure 10 at different instants of the analysis. The high convection occurring in the lateral face of the ice together with the incoming heat flux through the bottom wall are the main mechanisms that cause the motion of the phase-change front. These facts were also observed in the experience where the flow developed at the bottom of the ice rod promoted the clips release at about 4 min. The final volume of the ice is computed as 70 per cent of the original one; this value is similar to that observed in the measurements. A stratified temperature distribution is observed in the whole cavity with flat isotherm profiles. This thermal distribution is a feature typically found in natural convection studies of confined square cavities with high Rayleigh numbers (Ishikawa *et al.*, 2000). Based on a characteristic length of 0.1 m that corresponds to the height of water, a characteristic temperature variation of 15°C usually taken as the difference between the initial water temperature and the melting temperature, the resulting Rayleigh number for this case is 8.1×10^7. Since, the isotherm of 4°C (inversion temperature) remains close to the lateral edge of the ice, the inversion effects do not play a relevant role in the process. The largest temperature gradients are located at the phase-change interface and along the lower wall. Finally, the motion of the cold fluid current in the bottom of the cavity is perturbed by the hot incoming heat flux that generates some waves which, in turn, produces a complex flow pattern associated with the temperature distribution in this region (this last phenomenon was also observed in the experience).

To assess the performance of the FE-TB formulation proposed for the analysis when density inversion and isothermal phase-change phenomena are considered, a computation using the FV-HB model is also carried out for case C. The same space-time discretization is adopted for the current finite volume simulation. The experimental measurements together with the computed results for the temperature evolutions are shown in Figure 11. It is seen that both numerical predictions satisfactorily agree with the experimental measurements. In particular, slightly better results are computed with the FE-TB model at thermocouples 5, 6 and 7. Similar transient responses have been also found for the phase-change front position, isotherms and streamlines contours computed with the FE-TB and FV-HB models (results not shown).

4. Conclusions

Two different ice melting problems have been analysed using a fixed-mesh FE-TB formulation. The computed results have been found to be very similar to the

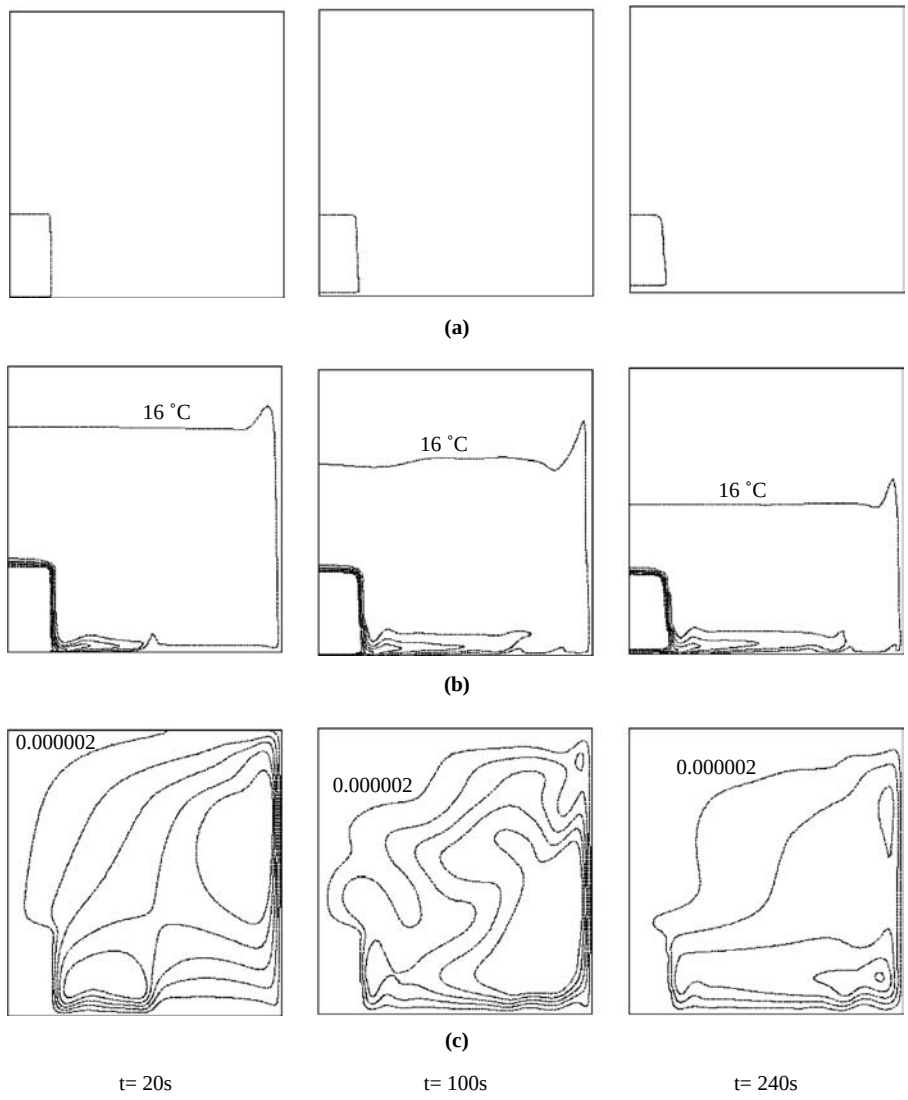

Figure 10.
Melting of a square rod of ice immersed in water

Notes: FE-TB results at different instants for case C. (a) Phase-change front position, (b) isotherms (plotted 2 ºC apart from 4 ºC to 16 ºC) and (c) streamlines (plotted 3.5×10^{-6} m^2/s apart from 2.0×10^{-6} m^2/s to 1.6×10^{-5} m^2/s).

corresponding predictions, also obtained in this study, provided by a finite volume enthalpy-based technique. Both numerical results, in turn, satisfactorily approached the available experimental measurements expressly conducted in the context of this work for validation purposes. Moreover, the natural convection together with the heat transfer boundary conditions have been observed to play an important role in the thermally coupled flow behaviour developed during the ice melting process.

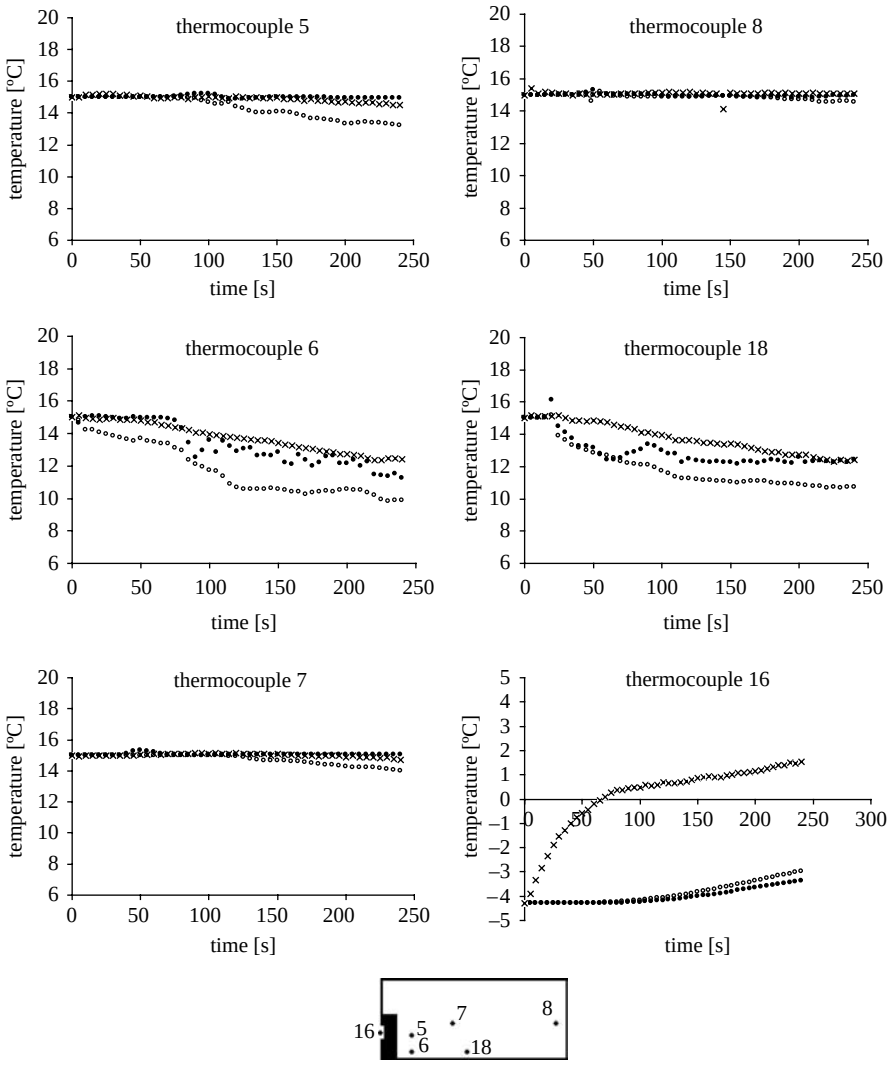

Figure 11.
Melting of a square rod of ice immersed in water

Notes: Experimental (×), FE-TB (●) and FV-HB (○) results for the temperature evolutions for case C

Further research will be focused on the improvement of the model (e.g. treatment of localised oscillations in the numerical response and consideration of volume changes owing to the solid-liquid transformation) and also on experimental tasks (e.g. additional temperature measurements in regions with strong convection, better control of the heat transfer conditions at the boundaries and implementation of a device to measure fluid velocities) with the final aim of getting more valuable data to achieve a more complete validation of the simulations.

References

Brent, A., Voller, V. and Reider, K. (1988), "Enthalpy-porosity technique for modelling convection-diffusion phase change", *Numerical Heat Transfer*, Vol. 13, pp. 297-318.

Celentano, D. (1998), "A finite element formulation for phase-change problems with advective effects", *Communications in Numerical Methods in Engineering*, Vol. 14, pp. 719-30.

Cruchaga, M. and Celentano, D. (2001), "A fixed-mesh finite element thermally coupled flow formulation for the numerical analysis of melting processes", *International Journal for Numerical Methods in Engineering*, Vol. 51, pp. 1231-58.

Cruchaga, M. and Celentano, D. (2005), "Numerical and experimental analysis of ice melting in water", in Idelsohn, S.R. and Sonzogni, V.E. (Eds), *Applications of Computational Mechanics in Structures and Fluids*, A Series of Handbooks on Theory and Engineering Applications of Computational Methods, CIMNE, Barcelona.

Dantzig, J. (1989), "Modeling liquid-solid phase changes with melt convection", *International Journal for Numerical Methods in Engineering*, Vol. 28, pp. 1769-85.

FLUENT Inc. (1999), *FLUENT® User's Guide – Release 5.3*, FLUENT Inc., Lebanon, NH.

Ishikawa, M., Hirata, T. and Noda, S. (2000), "Numerical simulation of natural convection with density inversion in a square cavity", *Numerical Heat Transfer*, Vol. 37, pp. 395-406.

Khodadadi, J. and Zhang, Y. (2001), "Effects of buoyancy-driven convection on melting within spherical containers", *International Journal of Heat and Mass Transfer*, Vol. 44, pp. 1605-18.

Lacroix, M. and Voller, V. (1990), "Finite difference solutions of solidification phase change problems: transformed versus fixed grids", *Numerical Heat Transfer, Part B*, Vol. 17, pp. 25-41.

Lewis, R. and Ravindran, K. (2000), "Finite element simulation of metal casting", *International Journal for Numerical Methods in Engineering*, Vol. 47, pp. 29-59.

McDaniel, D. and Zabaras, N. (1994), "A least-squares front-tracking finite element method analysis of phase change with natural convection", *International Journal for Numerical Methods in Engineering*, Vol. 37, pp. 2755-77.

Rieger, H. and Beer, H. (1986), "The melting process of ice inside a horizontal cylinder: effect of density anomaly", *Journal of Heat Transfer*, Vol. 108, pp. 166-73.

Swaminathan, C. and Voller, V. (1993), "On the enthalpy method", *International Journal of Numerical Methods for Heat and Fluid Flow*, Vol. 3, pp. 233-44.

Tsai, C., Yang, S. and Hwang, G. (1998), "Maximum density effect on laminar water pipe flow solidification", *International Journal of Heat and Mass Transfer*, Vol. 41, pp. 4251-7.

Webb, B. and Viskanta, R. (1986), "Natural-convection-dominated melting heat transfer in an inclined rectangular enclosure", *International Journal of Heat and Mass Transfer*, Vol. 29, pp. 183-92.

Yamada, M., Fukusako, S., Kawanami, T. and Watanabe, C. (1997), "Melting heat transfer characteristics of a horizontal ice cylinder immersed in quiescent saline water", *International Journal of Heat and Mass Transfer*, Vol. 40, pp. 4425-35.

Corresponding author
Marcela Cruchaga can be contacted at: mcruchag@lauca.usach.cl